Eur. Phys. J. C (2008) 57: 569–578
DOI 10.1140/epjc/s10052-008-0687-2

THE EUROPEAN PHYSICAL JOURNAL C

Regular Article - Theoretical Physics

AdS-QCD quark–antiquark potential, meson spectrum and tetraquarks

M.V. Carlucci[1,2], **F. Giannuzzi**[1,2,a], **G. Nardulli**[1,2], **M. Pellicoro**[1,2], **S. Stramaglia**[1,2]

[1]Università di Bari, 70126 Bari, Italia
[2]Sezione di Bari, I.N.F.N., 70126 Bari, Italia

Received: 16 May 2008 / Published online: 27 August 2008

Abstract The AdS/QCD correspondence predicts the structure of the quark–antiquark potential in the static limit. We use this piece of information together with the Salpeter equation (Schrödinger equation with relativistic kinematics) and a short range hyperfine splitting potential to determine quark masses and the quark potential parameters from the meson spectrum. The agreement between theory and experimental data is satisfactory, provided one considers only mesons comprising at least one heavy quark. We use the same potential (in the one-gluon-exchange approximation) and these data to estimate the constituent diquark masses. Using these results as input we compute tetraquark masses using a diquark–antidiquark model. The masses of the states $X(3872)$ or $Y(3940)$ are predicted rather accurately. We also compute tetraquark masses with open charm and strangeness. Our result is that tetraquark candidates such as $D_s(2317)$, $D_s(2457)$ or $X(2632)$ can hardly be interpreted as diquark–antidiquark states within the present approach.

PACS 12.39.Ki · 12.39.Pn · 12.90.+b

1 Introduction

Hadron spectroscopy has received in recent years renewed attention, both experimental and theoretical. On the experimental side several new charmonium and charmed states have been observed (for reviews see e.g. [1, 2]). The interpretation of the new states has triggered a considerable amount of theoretical work, especially so because some of the new states cannot be interpreted as ordinary quark–antiquark mesons (for reviews see [3, 4]). For some of the new states, such as the $X(3872)$ or $Y(3940)$ [5–11] an interpretation in terms of exotica (diquark–antidiquark bound states) has been given [12–15], using a refined version of the constituent quark model [16]. On the other hand also more conventional interpretations have been proposed. It is therefore useful to have an independent approach to the calculation of the tetraquark masses in order to assess the validity of the diquark–antidiquark interpretation of the new states. This is one of the aims of the present paper. We approach this problem using a semirelativistic method based on the use of a relativistic wave equation, the Salpeter equation. This is a Schrödinger equation with relativistic kinematics (for previous use of this equation for hadron spectroscopy see e.g. [17] and references therein); as such, it has the usual limitations of the static potential approach, but it presents the advantage of the relativistic kinematics.

A crucial point in this approach is the choice of the potential. There are several proposals in the literature; e.g. the Cornell potential [18] or its variants [19, 20]. We shall here use a modified version of a static quark potential, which has recently been found in the context of the AdS/QCD correspondence [21]. As shown in [21], this potential has the same behavior as expected from QCD, i.e. it is linearly rising at large distances while presenting Coulomb behavior at small distances. Clearly the interpolation between these two behaviors is phenomenologically relevant if it corresponds to length scales typical of the hadrons. This is a possible way to discriminate among the different models. Another aim of this paper is therefore to find the region where the AdS inspired potential differs from the usual QCD-based potentials and to see if it is of phenomenological significance. We fix the parameters of the model using, as input, data from the meson spectrum. We compare our results with the available experimental data for the mesonic spectrum and we find a reasonable good agreement. Once the parameters of the model are fixed, we can compute the diquark masses, i.e. a set of phenomenological parameters that we use, together with some additional hypotheses, to predict other spectra.

[a] e-mail: floriana.giannuzzi@ba.infn.it

The results of the paper are as follows. Assuming a diquark–antidiquark structure of tetraquark states, we find the masses for some of the X and Y states to be in reasonable agreement with experiment. The same procedure can be applied to tetraquarks comprising one charm quark and hidden strangeness. In this case the results are hardly compatible with the masses of possible tetraquark candidates, i.e. the states $D_s(2317)$ [22], $D_s(2457)$ [22] and $X(2632)$ [23].

The paper is organized as follows. In Sect. 2 we describe the model, introducing the Salpeter equation, the potential term and the numerical method adopted to solve the wave equation. In Sect. 3 we determine the parameters of our model fitting the meson spectra; the results allow for a comparison with the presently available meson data. In Sect. 4 the constituent diquark masses are calculated in the one-gluon-exchange approximation. In Sect. 5 we compute the spectra of a few tetraquark states. Finally, in Sect. 6 we draw our conclusions.

2 Wave equation and the central potential

The wave equation we shall use in this paper is an eigenvalue equation for the Hamiltonian of two point-like particles, taking into account the relativistic kinematics. It is known in the literature as the Salpeter equation. In QCD it arises from the Bethe–Salpeter equation replacing the interaction with an instantaneous local potential $V(r)$ and considering a limited Fock space containing $q\bar{q}$ pairs only. We write the Salpeter equation for a meson comprising a quark and an antiquark in the meson rest frame as follows ($\hbar = c = 1$):

$$\left(\sqrt{m_1^2 - \nabla^2} + \sqrt{m_2^2 - \nabla^2} + V(r)\right)\psi(\mathbf{r}) = M\psi(\mathbf{r}). \tag{1}$$

For a central potential, one can search for energy eigenfunctions with definite angular momentum ℓ, thus writing

$$\psi(\mathbf{r}) = Y_{\ell m}(\hat{\mathbf{r}})\phi_\ell(r). \tag{2}$$

The radial wavefunction $\phi_\ell(r)$ satisfies

$$\frac{2}{\pi}\int_0^{+\infty} \mathrm{d}r' r'^2 \int_0^{+\infty} \mathrm{d}k \left(\sqrt{k^2+m_1^2} + \sqrt{k^2+m_2^2}\right) \times k^2 j_\ell(kr) j_\ell(kr')\phi_\ell(r') = \left[M - V(r)\right]\phi_\ell(r), \tag{3}$$

where $j_\ell(x)$ are spherical Bessel functions. For $\ell = 0$, $j_0(x) = \sin x/x$, and the Salpeter equation reduces to

$$\frac{2}{\pi}\int_0^{\infty} \mathrm{d}r' \int_0^{\infty} \mathrm{d}k \left(\sqrt{k^2+m_1^2} + \sqrt{k^2+m_2^2}\right) \times \sin(kr)\sin(kr')u_0(r') = \left[M - V(r)\right]u_0(r), \tag{4}$$

where

$$u_0(r) = r\phi_0(r). \tag{5}$$

Let us discuss the potential energy. The potential $V(r)$ that we adopt comprises two parts:

$$V(r) = V_{\mathrm{AdS}}(r) + V_{\mathrm{spin}}(r). \tag{6}$$

$V_{\mathrm{AdS}}(r)$ describes the central term of the potential, i.e. it contains its linearly confining part at large distances and the short distance behavior predicted by perturbative QCD. For $V_{\mathrm{AdS}}(r)$ we use a slightly modified version of the potential obtained by Andreev and Zakharov [21] in the framework of the gauge/string duality approach [24–26]. $V_{\mathrm{spin}}(r)$ is the hyperfine term to be discussed below.

2.1 Static quark potential

In the gauge/string duality approach [24–26] the expectation value of the Wilson loop is given by

$$\langle W(\mathcal{C})\rangle \sim \mathrm{e}^{-S}, \tag{7}$$

where S is the area of a string world-sheet bounded by a curve $\mathcal{C}$ at the boundary of the AdS space (for references to the original papers see also [27–32]). To compute the potential the authors start with the Nambu–Goto action

$$S = \frac{1}{2\pi\alpha'}\int \mathrm{d}^2\xi \sqrt{\det G_{nm}\partial_\alpha X^n \partial_\beta X^m}, \tag{8}$$

with the following background metric in $D = 5$:

$$\mathrm{d}s^2 = G_{nm}\mathrm{d}X^n\mathrm{d}X^m = R^2\frac{h}{z^2}\left(\mathrm{d}x^i\mathrm{d}x^i + \mathrm{d}z^2\right), \quad h = \exp\frac{cz^2}{2}, \tag{9}$$

where $i = 0, \ldots, 3$. Choosing in (8) $\xi^1 = t$ and $\xi^2 = x$, (8) becomes

$$S = \frac{g}{2\pi}T\int_{-\frac{r}{2}}^{+\frac{r}{2}} \mathrm{d}x \frac{h}{z^2}\sqrt{1 + \left(\frac{\mathrm{d}z}{\mathrm{d}x}\right)^2}, \tag{10}$$

where $g = \frac{R^2}{\alpha'}$. From this action one can obtain an equation of motion for the variable z, from which an expression for the interquark distance r is derived as follows [21]:

$$r(\lambda) = 2\sqrt{\frac{\lambda}{c}}\int_0^1 \mathrm{d}v\, v^2 \exp^{\lambda(1-v^2)/2} \times \left(1 - v^4 \exp^{\lambda(1-v^2)}\right)^{-1/2}. \tag{11}$$

This expression depends on the constant c; λ is a parameter in the range $]0, 2[$. In terms of the original parameters it is given by $\lambda = cz_0^2$, with z_0 the value of the fifth coordinate, z, in $x = 0$.

The potential is obtained by computing the energy of the configuration; first one changes the integration variable from x to z in (10); the resulting integral is divergent at $z = 0$ and has to be regularized. The finite part gives

$$E(\lambda) = \frac{g}{\pi}\sqrt{\frac{c}{\lambda}}\left(-1 + \int_0^1 \mathrm{d}v v^{-2} \times \left[\exp^{\lambda v^2/2}\left(1 - v^4 \exp^{\lambda(1-v^2)}\right)^{-1/2} - 1\right]\right). \quad (12)$$

This is the potential given in [21]. The dependence $E(r)$ is obtained by elimination of the parameter λ between (11) and (12); $E(r)$ depends on the two parameters g and c.

Our potential $V_{\mathrm{AdS}}(r)$ is given as follows:

$$V_{\mathrm{AdS}}(r) = \begin{cases} E(r) + V_0, & r > r_m, \\ E(r_m) + V_0, & r \le r_m. \end{cases} \quad (13)$$

This phenomenological procedure, which has allowed one to get an expression for the QCD potential with the expected properties, is known as the bottom-up approach of the AdS/QCD correspondence. According to it, starting from QCD, one constructs its dual theory in such a way as to reproduce some properties of QCD. Besides the QCD potential, many results have been obtained so far, such as the determination of the numerical values of some observables [33], in good agreement with the experimental data, or the linearity of the Regge trajectories [34, 35].

The expression (12) derives from the metric (9); we have also tried to use a slight modification of the dilaton term in (9), specifically, changing the power of z at the exponent. We find that, for any power of z, the potential has the same behavior, i.e. Coulomb-like for small r and linearly rising for large r. As far as the QCD potential is concerned they are all possible candidates for the AdS metric of the QCD dual space.

We have introduced a constant term V_0 in the potential. This is allowed, because the more general string action is obtained by adding to the Nambu–Goto action a term

$$\delta S = C_R \int \mathrm{d}^2\xi\, R\sqrt{\det G_{nm}\partial_\alpha X^n \partial_\beta X^m}, \quad (14)$$

where R is the scalar curvature. One can easily prove that adding δS to S corresponds to adding a constant term to the interquark potential.

Another modification appearing in (13) is the introduction of a cutoff at short distances $r \le r_m$ [17]. The reason lies in the use of the relativistic kinematics embodied in (1). As a matter of fact, the potential $E(\lambda)$ in (12) diverges as $\lambda \to 0$. It is a Coulombic divergence occurring at $r \to 0$, because the small distance region corresponds to $\lambda \to 0$. This divergence is harmless if one uses the Schrödinger equation for the wavefunction, but in the case of the Salpeter equation (1) it produces an unphysical logarithmic divergence for the S-wave wavefunction for $r \to 0$. To cure this unphysical singularity arising from the static approximation one assumes a constant potential for r smaller than

$$r_m \sim \frac{1}{M}. \quad (15)$$

The proportionality constant can be fixed using quark duality arguments [36], which show that one expects different results for the equal and unequal mass cases. Thus we use

$$\begin{aligned} r_m &= \frac{k}{M} \quad (m_1 = m_2), \\ r_m &= \frac{k'}{M} \quad (m_1 \ne m_2). \end{aligned} \quad (16)$$

This concludes the discussion of the central part of the potential.

2.2 Spin term

Let us now discuss the spin term. In the approximation of one-gluon-exchange one knows that the spin term is enhanced at short distances and is proportional to the inverse quark masses. Following [37], we use

$$V_{\mathrm{spin}}(r) = A\frac{\tilde{\delta}(r)}{m_1 m_2}\mathbf{S_1}\cdot\mathbf{S_2}, \quad (17)$$

where $\tilde{\delta}$ is a function enhanced at small distances. In the constituent quark model the constant A is proportional to α_s, which is the running coupling constant, so we have introduced two different parameters for mesons containing at least one charm and one bottom quark (A_c and A_b, respectively). We adopt the smeared delta function used in [37]:

$$\tilde{\delta}(r) = \left(\frac{\sigma}{\sqrt{\pi}}\right)^3 \mathrm{e}^{-\sigma^2 r^2}. \quad (18)$$

The potential depends therefore on eight parameters: c, g, V_0, k, k', A_c, A_b and σ. Moreover, we have to fix the constituent quark masses: $m_u = m_d \equiv m_q$, m_s, m_c and m_b.

2.3 Numerical solutions

To solve (1) we use the Multhopp method [38], which, as shown in [17], is particularly useful for equations of the form considered here. By this method one transforms the integral equation into a set of linear equations introducing N parameters θ_k, called Multhopp's angles. The set of equations is as follows [17]:

$$\sum_{m=1}^{N} B_{km}\psi(\theta_k) = M\psi(\theta_m), \quad (19)$$

where $\psi(\theta_k) = u_0(-\cot\theta_k)$, $\theta_k = \frac{k\pi}{N+1}$ $(k = 1, \ldots, N)$ and

$$B_{km} = \frac{2}{N+1}\sum_{j=1}^{N}\sin(j\theta_m)I_{jk} \tag{20}$$

with

$$\begin{aligned} I_{jk} = {} & -\frac{2}{\pi}\lim_{\epsilon\to 0}\left\{\int_0^{\theta_k-\epsilon}\frac{\mathrm{d}\theta\sin j\theta}{\sin^2\theta(\cot\theta-\cot\theta_k)^2}\right. \\ & \left. + \int_{\theta_k+\epsilon}^{\pi}\frac{\mathrm{d}\theta\sin j\theta}{\sin^2\theta(\cot\theta-\cot\theta_k)^2} - \frac{2}{\epsilon}\sin^2\theta_k\sin j\theta_k\right\} \\ & + \frac{2}{\pi}\int_0^{\pi}\frac{\mathrm{d}\theta\sin j\theta}{\sin^2\theta}\left[\frac{1}{(\cot\theta-\cot\theta_k)^2}\right. \\ & - \frac{1}{2|\cot\theta-\cot\theta_k|}\big(m_1K_1\big(m_1|\cot\theta-\cot\theta_k|\big) \\ & \left. + (m_1\leftrightarrow m_2)\big)\right]. \end{aligned} \tag{21}$$

Notice that the way of writing in (21) makes explicit the prescription to avoid the divergence in the integral both for the massive and the massless case; $K_1(x)$ is the modified Bessel function.

3 Meson spectrum

The strategy we follow to evaluate the parameters of the model is to estimate them by using information from the meson spectra. Subsequently, in the next sections we use this information to fit diquark masses and, from these data, tetraquark masses. In principle, one might follow a different strategy, using all available experimental data to get a best fit of the parameters. We have not followed this approach, because to get the spectrum of diquarks and tetraquarks we make further assumptions, e.g. the use of the quark–quark potential as obtained by the one-gluon-exchange approximation.

Therefore, after having fixed the parameters from the mesonic spectrum, we shall use below experimental data for the X and Y states to test the hypothesis of the diquark–antidiquark structure of these exotica.

In order to get the numerical values for the parameters ($c, g, V_0, k, k', A_c, A_b, \sigma$, $m_u = m_d \equiv m_q$, m_s, m_c and m_b) we use the Salpeter equation for the mesons with both $J^P = 0^-$ and 1^-. We consider only mesons containing at least one heavy (c, b) quark, because we expect that the approximation of a static potential works better for these states. The set of available data comprises about 20 masses. The results of the best fit are reported in Table 1 for heavy mesons. They correspond to the following set of parameters:

$$\begin{aligned} & c = 0.3\ \mathrm{GeV}^2, \quad g = 2.75, \quad V_0 = -0.49\ \mathrm{GeV}, \\ & A_c = 7.92\ \mathrm{GeV}^3, \quad A_b = 3.09\ \mathrm{GeV}^3, \\ & k = 1.48, \quad k' = 2.15, \quad \sigma = 1.21\ \mathrm{GeV}^2, \\ & m_q = 0.302\ \mathrm{GeV}, \quad m_s = 0.454\ \mathrm{GeV}, \\ & m_c = 1.733\ \mathrm{GeV}, \quad m_b = 5.139\ \mathrm{GeV}. \end{aligned} \tag{22}$$

In order to test the limits of the model we also compute the masses of states containing only light (u, d and s) quarks. The results for their spin averaged masses are shown in Table 2. For the lightest mesons we find a large deviation, while such a discrepancy is somewhat reduced in the case of $s\bar{s}$ and for higher radial excitations. This is reasonable, since the constituent quark model with instantaneous interaction is not able to describe the chiral dynamics of light states. The better accuracy of the $s\bar{s}$ system allows us to fix the spin constant A_s in (17) from this channel, obtaining $A_s = 11.3$ GeV^3, which will be used in the calculation of the masses of the lightest diquarks. With this value, we obtain for φ a mass $m = 1.011$ GeV (the experimental value is 1.019 GeV) and for φ' a mass $m = 1.663$ GeV (the experimental value is 1.680 GeV).

It might be useful at this stage to study the effect of the relativistic kinematics on the equation of state. To this end we have used the same potential, with the values of parameters indicated by (22) with two different equations: the Salpeter equation (1) and the Schrödinger equation. The results of the two equations for mesons with $J^P = 1^-$ are reported in Table 3. The comparison between the two computed spectra and the experimental one shows that, as expected, the results obtained by the Salpeter equation are more accurate than the ones obtained by the Schrödinger equation. We conclude that the advantage of using the Salpeter equation is particularly significant for the charmed states, since this equation takes into account a relevant source of corrections, i.e. those due to the relativistic kinematics.

A final comment concerns the use of the AdS/QCD inspired potential. As we stressed in the introduction, many potentials have been used in the literature to fit the meson spectra. If they have to reproduce the constraints of QCD they must rise linearly at large distances and have a Coulomb-like behavior at small r. We wish to compare the potential we have used, i.e. $V_{\mathrm{AdS}} = E(r) + V_0$ in (13), with a typical QCD inspired potential, i.e. the Richardson potential [19]:

$$V_R(r) = \frac{8\pi}{33-2n_f}\Lambda\left(\Lambda r - \frac{f(\Lambda r)}{\Lambda r}\right) + V_1, \tag{23}$$

Table 1 Mass spectra for heavy mesons; $q = u, d$. A star (*) means that this state needs confirmation. Units are GeV

Flavor	Level	$J = 0$			$J = 1$		
		Particle	Th. mass	Exp. mass [39]	Particle	Th. mass	Exp. mass [39]
$c\bar{q}$	$1S$	D	1.862	1.867	D^*	2.027	2.008
	$2S$		3.393			2.598	2.622
	$3S$		2.837			2.987	
$c\bar{s}$	$1S$	D_s	1.973	1.968	D_s^*	2.111	2.112
	$2S$		2.524			2.670	
	$3S$		2.958			3.064	
$c\bar{c}$	$1S$	η_c	2.990	2.980	J/ψ	3.125	3.097
	$2S$		3.591	3.637		3.655	3.686
	$3S$		3.994			4.047	4.039
$b\bar{q}$	$1S$	B	5.198	5.279	B^*	5.288	5.325
	$2S$		5.757			5.819	
	$3S$		6.176			6.220	
$s\bar{b}$	$1S$	B_s	5.301	5.366	B_s^*	5.364	5.412
	$2S$		5.856			5.896	
	$3S$		6.266			6.296	
$b\bar{c}$	$1S$	B_c	6.310	6.286	B_c^*	6.338	6.420
	$2S$		6.869			6.879	
	$3S$		7.221			7.228	
$b\bar{b}$	$1S$	η_b	9.387	9.300*	Υ	9.405	9.460
	$2S$		10.036			10.040	10.023
	$3S$		10.369			10.371	10.355
	$4S$		10.619			10.620	10.579

Table 2 Mass spectra for the spin averaged masses of the light mesons; $q = u, d$. Units are GeV

Flavor	Level	Th. mass	Exp. mass [39]
$q\bar{q}$	$1S$	0.792	0.616
	$2S$	1.386	1.424
$q\bar{s}$	$1S$	0.932	0.794
	$2S$	1.501	
$s\bar{s}$	$1S$	0.981	0.912
	$2S$	1.571	≈1.653

where Λ is a parameter, $n_f = 3$ is the number of flavors, and

$$f(t) = \frac{4}{\pi} \int_0^\infty \mathrm{d}q \, \frac{\sin(qt)}{q} \left(\frac{1}{\ln(1+q^2)} - \frac{1}{q^2} \right). \qquad (24)$$

To allow for a comparison, similarly to what we have done for the AdS potential, we have added a constant term V_1 to the original Richardson potential. We fix the value of Λ and V_1 imposing the requirement that the linearly confining parts of V_{AdS} and V_R coincide at large r. For V_{AdS} we use the fit obtained by the meson spectrum; this gives for Λ and V_1 the values $\Lambda = 0.44$ GeV and $V_1 \sim -0.6$ GeV.

We are now able to compare the two potentials, and the result can be found in Fig. 1. It shows that, even though the two potentials almost coincide asymptotically, they differ significantly in the intermediate region, which is the region of interest from a phenomenological point of view.

4 Diquark masses

In view of the applications to be discussed in the subsequent sections we wish to derive a set of parameters, which we call *effective diquark masses* or simply diquark masses.

In the one-gluon-exchange approximation the color antisymmetric channel corresponding to the antitriplet in the decomposition

$$3 \otimes 3 = \bar{3} \oplus 6 \qquad (25)$$

Table 3 Comparison of spectra for mesons with $J^P = 1^-$ computed by the Salpeter equation in (1) and the Schrödinger equation. The same potential $V(r)$ is used in both cases

Flavor	Level	Salpeter	Schrödinger
$c\bar{q}$	1S	2.027	2.154
	2S	2.598	2.877
$c\bar{s}$	1S	2.111	2.182
	2S	2.670	2.843
$c\bar{c}$	1S	3.125	3.133
	2S	3.655	3.695
$b\bar{q}$	1S	5.288	5.494
	2S	5.819	6.204
$s\bar{b}$	1S	5.364	5.507
	2S	5.896	6.154
$b\bar{c}$	1S	6.338	6.550
	2S	6.879	6.922
$b\bar{b}$	1S	9.405	9.774
	2S	10.040	10.055

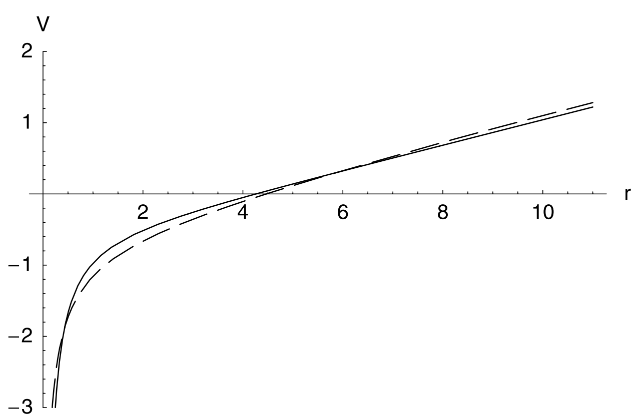

Fig. 1 Comparison between the AdS/QCD inspired potential $V_{\text{AdS}}(r)$ (*solid line*) and the Richardson potential [19] $V_R(r)$ (*dotted line*). For the values of the parameters see the text. Units are GeV (V) and GeV^{-1} (r)

is attractive. Moreover, in the same approximation the attractive potential between the two quarks QQ is half the one between a quark Q and an antiquark $\bar{Q}$. We therefore adopt, as usual, the following value for the potential between the two quarks comprising the diquark:

$$V_{QQ} = \frac{1}{2} V_{Q\bar{Q}}. \tag{26}$$

However, it must be kept in mind that this approximation holds only for the QCD perturbative interaction and might be modified in the linearly confining part. Therefore, we expect that it works better for heavy diquarks, as, in this case, the interaction explores smaller distances than for light diquarks.

To derive the diquark effective masses we use the Salpeter equation with the same set of parameters used to fit the meson spectrum. Also in this case, as for mesons, one sees that the spin term works differently for $S = 1$ and $S = 0$ states. It adds a positive contribution for $S = 1$ and subtracts the same contribution multiplied by a factor of -3 for $S = 0$.

The results are reported in Table 4; diquarks with $S = 0$ are denoted as $[QQ]$, those with $S = 1$ as $\{QQ\}$. We have also reported the results of a different fit found by the authors of [40, 41] who use a quasipotential of the Schrödinger type [42]. We also note that in a series of papers [12–15], Maiani and collaborators have put forward an interpretation of the new X and Y states, as well as of light scalars such as $\sigma(480)$, $\kappa(800)$, $f_0(980)$, etc., as four-quark states comprising a diquark and an antidiquark (see below). They use a quark constituent model similar to the well known De Rujula–Georgi–Glashow model [16]. Also in [12–15] an effective diquark mass is used; however, its meaning is different from ours, because the constituent quark mass used in these papers takes into account both the average kinetic energy and the potential energy, differently from our case, where a wave equation is considered. Therefore, no numerical comparison is possible among our values for diquark masses and those found in [12–15].

5 Tetraquark spectrum

In this section we wish to discuss the possibility that two diquarks, more precisely a diquark and an antidiquark, combine to produce a tetraquark state. Such an interpretation was advanced long ago in order to give an interpretation of the light scalars $a_0(980)$ and $f_0(980)$ in terms of constituent quarks [43–45]. The recent discovery of new states, with both hidden and open charm, has raised a new interest for this model, though the interpretation of the new states is controversial, see for reviews [3] and [4].

Let us start with the state $X(3872)$ [5–10]. The average mass of this state is 3871.2 ± 0.4 MeV and its quantum numbers should be $J^{PC} = 1^{++}$. The assignment $C = +1$ follows from the fact that the decay $X \to \gamma J/\Psi$ is observed. Moreover, the decay $X \to \pi^+\pi^- J/\Psi$ is also observed; the part of the 2π invariant mass spectrum that can be ascribed to a ρ^0 decay is consistent with S-wave decay of the X state. From this the assignment $P = +1$ follows. Finally, the angular distribution in this channel is incompatible with $J = 0$ and therefore the only remaining possibilities are $J = 1$ and $J = 2$. If the peak in the $D^0\bar{D}^0\pi^0$ decay channel at 3875.4 MeV (at 2σ from the mass of $X(3872)$) is interpreted as due to this state, then the $J = 2$ should be excluded, which leaves us with $J = 1$ only.

Table 4 Diquark masses. The masses of the present paper are obtained by the Salpeter equation (see text). The model in [40, 41] uses a quasipotential of the Schrödinger type [42]. $\{QQ\}$ (respectively $[QQ]$) means a spin 1 (respectively $S=0$) diquark QQ. Units are GeV

State	Mass (this paper)	Mass [40, 41]	Mass	Mass (this paper)	Mass [40, 41]
$\{qs\}$	0.980	1.069	$[qs]$	0.979	0.948
$\{ss\}$	1.096	1.203			
$\{cq\}$	2.168	2.036	$[cq]$	2.120	1.973
$\{cs\}$	2.276	2.158	$[cs]$	2.235	2.091
$\{cc\}$	3.414	3.226			
$\{bq\}$	5.526	5.381	$[bq]$	5.513	5.359
$\{bs\}$	5.630	5.482	$[bs]$	5.619	5.462
$\{bc\}$	6.741	6.526	$[bc]$	6.735	6.519
$\{bb\}$	10.018	9.778			

Several interpretations have been proposed for this state. Since the mass of this state almost coincides with the sum of the masses of the D^0 and $\bar{D}^{*0}$ states, a natural explanation is that of a molecular state comprising the two charmed mesons [46–51]. The interpretation as a χ'_{c1} state [52] is unlikely because of the small value of the ratio $\frac{\mathcal{B}(X\to\gamma J/\Psi)}{\mathcal{B}(X\to\pi^+\pi^- J/\Psi)}$ and because of the value of the mass. Also the interpretation as a $c\bar{c}g$ hybrid [53] is difficult due to the fact that lattice data predict larger masses for these states (for a discussion and for a comprehensive list of other models, see [3]).

As mentioned above, another possibility is that this state comprises four quarks. They might be a four-quark cluster without internal structure [54] or a bound state of two diquarks, as first discussed in [13] and more recently in [41]. We shall return to this interpretation below.

The Belle Collaboration observes two bumps, at 3940 MeV. They do not necessarily correspond to two different states. The state called $Y(3940)$ is observed in the decay mode $B \to K\omega J/\Psi$ [11]. Its reported mass is $M = 3943 \pm 11 \pm 13$ MeV. Its interpretation as a charmonium $c\bar{c}$ state is possible, but it should be corroborated by the observation of the decay mode $Y \to D^{(*)}\bar{D}^{(*)}$, which has not yet been seen. Also the interpretation as a $c\bar{c}$ gluon has been proposed, though the predicted mass of such a state, around 4.3–4.5 GeV from lattice QCD computations [55, 56], is significantly larger than the measured value. Also in this case a four-quark interpretation is possible; in particular, the state might be the 2^{++} state predicted by the diquark–antidiquark scheme [13]. The other state $X(3940)$ needs confirmation; it is observed [57] in double charm production: $e^+e^- \to J/\psi X \to J/\psi D\bar{D}^*$. Its possible interpretations are the states χ'_c or η''_c [3].

We wish to test the interpretation of these states as diquark–antidiquark bound states, in the same spirit as [12–15] and [40]. Note however that our approach is different from that followed in these papers. As a matter of fact we apply a wave equation for the tetraquark states, comprising the diquarks (Q_1Q_2) and $(\bar{Q}_3\bar{Q}_4)$, as follows:

$$\left(\sqrt{m_{12}^2-\nabla^2}+\sqrt{m_{34}^2-\nabla^2}+\tilde{V}(R)\right)\psi_t(\mathbf{R}) = M_t\psi_t(\mathbf{R}). \tag{27}$$

Here M_t and $\psi_t(\mathbf{R})$ are the tetraquark mass and wavefunction, respectively; m_{ij} is the effective diquark mass computed above. R is the distance between the centers of the two diquarks. We take into account the structure of the diquarks by defining a smeared potential as follows:

$$\tilde{V}(R) = \frac{1}{N}\int d\mathbf{r_1}\int d\mathbf{r_2}\left|\psi(\mathbf{r_1})\right|^2\left|\psi(\mathbf{r_2})\right|^2 V\left(|\mathbf{R}+\mathbf{r_1}-\mathbf{r_2}|\right) \tag{28}$$

with

$$N = \int d\mathbf{r_1}\int d\mathbf{r_2}\left|\psi_{12}(\mathbf{r_1})\right|^2\left|\psi_{34}(\mathbf{r_2})\right|^2. \tag{29}$$

In these equations $\psi_{12}(\mathbf{r_1})$ (respectively $\psi_{34}(\mathbf{r_2})$) is the wavefunction of the diquark whose content is Q_1Q_2 (respectively Q_3Q_4); for $V(r)$ we use (6), and the masses appearing in the spin term of (17) are diquark masses. In this paper we only consider a diquark with internal orbital quantum number $\ell = 0$; therefore, ψ_{ij} is related to $u_0(r)$ defined above as follows: $\psi_{ij}(\mathbf{r}) = \frac{u_0(r)}{r}$.

Since $|\psi_{12}(\mathbf{r})|^2$ is strongly peaked at $r \sim 0$ (see Fig. 2) we cut off the integrals in (28) and (29) at $r_{1,2} \le R_0$ where R_0 is the peak value of $u_{0t}(r)$, the wavefunction of the tetraquark. This procedure ensures that the two diquarks are on average inside the tetraquark's bag. In Fig. 3 is represented $u_{0t}(r)$ for the tetraquark $[cq]\{\bar{c}\bar{q}\}$.

We finally note that we use for $\psi_{12}(\mathbf{r})$ the result obtained from the diquark wave equation. This is only approximately correct because that equation provides the diquark wavefunction in the diquark rest frame, whereas (27) holds in the tetraquark rest frame. However, for diquarks comprising heavy quarks (c, b) the average diquark velocity is small

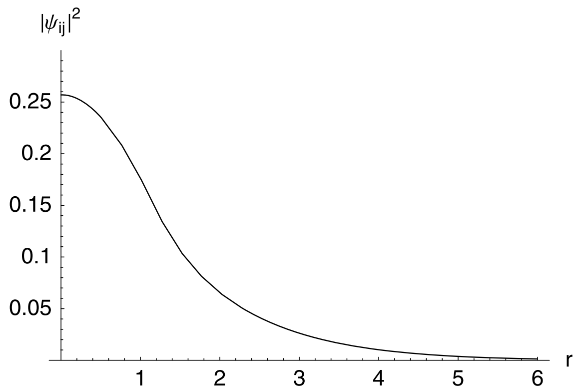

Fig. 2 The squared diquark wavefunction (in GeV^3) versus r (in GeV^{-1}). The data correspond to the diquark $[cq]$

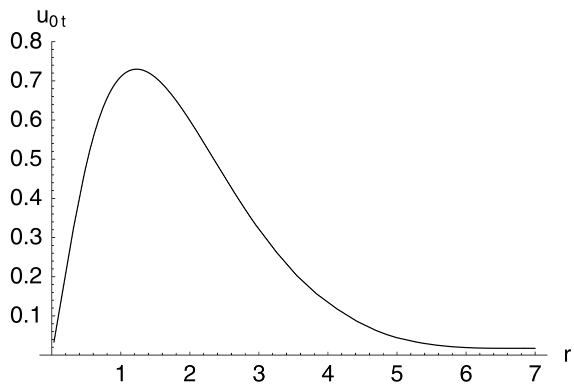

Fig. 3 The tetraquark wavefunction $u_{0t}(r)$ (in $\text{GeV}^{1/2}$) versus r (in GeV^{-1}). The data correspond to the tetraquark $[cq]\{\bar{c}\bar{q}\}$

(we estimate $\beta \sim 0.15$ for diquarks with open charm and $\beta \sim 0.06$ for diquarks with open bottom). Therefore, we can neglect the distortion induced by the Lorentz boost on the wavefunction. The effect of convoluting the potential with the wavefunctions in (28) is shown in Fig. 4.

In Tables 5 and 6 we present our predictions for the four-quark states with hidden charm and hidden bottom, respectively. Notice that we have adopted the same values of the free parameters used in the previous sections, so basically our calculation is parameter-free. It is remarkable that in the two cases that a comparison with experiment is possible, our results agree, within the errors, with the data. A further comment is the following. A peculiar feature of the diquark–antidiquark scheme for the X state is the prediction of four different states with mass differences of a few MeV. Two of them are neutral: $X_u = [cu][\bar{c}\bar{u}]$, $X_d = [cd][\bar{c}\bar{d}]$, and two charged: $X^+ = [cu][\bar{c}\bar{d}]$, $X^- = [cd][\bar{c}\bar{u}]$. It is possible that the two states seen through the decay modes $J/\psi\pi^+\pi^-$ and $D^0\bar{D}^0\pi^0$ are really different and they would correspond to the neutral states X_u and X_d, since the mass difference between the two bumps at 3871 and 3876 MeV is of the same order of magnitude as the mass difference between the u and

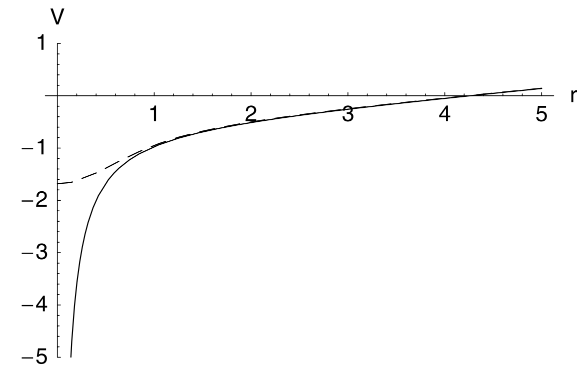

Fig. 4 The potential between static diquarks (*dashed line*) and its modification according (28) (*solid line*). Units are GeV (V) and GeV^{-1} (r). The data refer to the $[cq]\{\bar{c}\bar{q}\}$ potential

d quarks. According to [15] this is a piece of evidence in favor of the four-quark interpretation of these states. We have not included any mass difference between u and d quarks, but also in our scheme one would expect a mass difference of a few MeV between the two neutral states. We note that in [15] a strategy to find the two missing charged partners is delineated. We refer to this paper for further details.

By our model we can compute also radial excitations of tetraquarks. For example, the first radial excitations of the two X states with 1^{+-} have mass $m = 4.421$ GeV and $m = 4.418$ GeV, respectively. In [58] the state $Z(4433)$, recently observed by the Belle Collaboration [59] through the decay $Z(4433) \to \psi(2S)\pi^\pm$, is interpreted as the first radial excitation of one of these states. Although the difference between theory and experiment in this case is larger than, say, for $X(3872)$ or $Y(3940)$, this interpretation is compatible with our results because of the theoretical errors of the present model. Another exotic state is $Y(4260)$, found by the BaBar Collaboration [60] and confirmed by CLEO [61] and BELLE [62]. It is interpreted in [14] as an orbital excitation of a tetraquark state, an interpretation we are neither able to confirm nor to disprove, as we have limited the analysis to the $\ell = 0$ states.

Let us now comment on the light tetraquarks. We do not include them in the tables because for them the assumptions of our model and therefore its results are less reliable; moreover, as discussed in connection with (28) and (29), the distortion of the diquark wavefunction due to the relativistic motion is larger for light diquarks and its neglect generates a greater error.

Let us finally comment on the possible existence of tetraquarks comprising a heavy diquark and a light diquark. We present in Table 7 our predictions for tetraquarks with open charm and strangeness and compare them with the prediction of the constituent quark model of [13]. In [13] the state 0^+ is associated with the particle $D_s(2317)$ [22], 1^+ with $D_s(2457)$ [22] and 2^+ with $X(2632)$ [23]. Our results are significantly different from those of [13]. Again,

Table 5 Four-quark states with hidden charm interpreted as bound states comprising a diquark (cq) and an antidiquark ($\bar{c}\bar{q}$). $\{QQ\}$ (respectively $[QQ]$) means a spin 1 (respectively spin 0) diquark QQ. The masses of the present paper are obtained by the Salpeter equation (see text). The model in [40, 41] uses a quasipotential of the Schrödinger type [42]. Reference [13] uses a constituent quark model († means that the experimental value is used as input in this case). Units are GeV

J^{PC}	Flavor content	Mass (this paper)	Mass [40, 41]	Mass [13]	Exp. State	Exp. mass
0^{++}	$[cq][\bar{c}\bar{q}]$	3.857	3.812	3.723		
1^{++}	$([cq]\{\bar{c}\bar{q}\}+[\bar{c}\bar{q}]\{cq\})/\sqrt{2}$	3.899	3.871	$3.872^{\dagger}$	$X(3872)$	3.8712 ± 0.0004 [5–10]
1^{+-}	$([cq]\{\bar{c}\bar{q}\}-[\bar{c}\bar{q}]\{cq\})/\sqrt{2}$	3.899	3.871	3.754		
0^{++}	$\{cq\}\{\bar{c}\bar{q}\}$	3.729	3.852	3.832		
1^{+-}	$\{cq\}\{\bar{c}\bar{q}\}$	3.833	3.890	3.882		
2^{++}	$\{cq\}\{\bar{c}\bar{q}\}$	3.988	3.968	3.952	$Y(3940)$	$3.943 \pm 0.011 \pm 0.013$ [11]

Table 6 Four-quark states with hidden bottom interpreted as bound states comprising a diquark (bq) and an antidiquark ($\bar{b}\bar{q}$). $\{QQ\}$ (respectively $[QQ]$) means a spin 1 (respectively $S=0$) diquark QQ. The masses of the present paper are obtained by the Salpeter equation (see text). The model in [40, 41] uses a quasipotential of the Schrödinger type [42]. Units are GeV

J^{PC}	Flavor content	Mass (this paper)	Mass [40, 41]
0^{++}	$[bq][\bar{b}\bar{q}]$	10.260	10.471
$1^{+\pm}$	$([bq]\{\bar{b}\bar{q}\}\pm[\bar{b}\bar{q}]\{bq\})/\sqrt{2}$	10.284	10.492
0^{++}	$\{bq\}\{\bar{b}\bar{q}\}$	10.264	10.473
1^{+-}	$\{bq\}\{\bar{b}\bar{q}\}$	10.275	10.484
2^{++}	$\{bq\}\{\bar{b}\bar{q}\}$	10.296	10.534

Table 7 Comparison between the results of the present model and those of [13] for tetraquarks with open charm and strangeness. Units are GeV

J^P	Flavor content	Th. mass (this paper)	Th. mass (model [13])
0^+	$[cq][\bar{q}\bar{s}]$	2.840	2.371
0^+	$\{cq\}\{\bar{q}\bar{s}\}$	2.503	2.424
1^+	$\{cq\}[\bar{q}\bar{s}]$	2.880	2.410
1^+	$\{cq\}\{\bar{q}\bar{s}\}$	2.748	2.462
1^+	$[cq]\{\bar{q}\bar{s}\}$	2.841	2.571
2^+	$\{cq\}\{\bar{q}\bar{s}\}$	2.983	2.648

this might be due to the limitations of one or both of the constituent quark models. In any event, on the basis of the results in Sect. 3 we do not expect theoretical errors larger than a few hundred MeV for the results of the present model in Table 7, so that we do not support the interpretation of the states $D_s(2317)$, $D_s(2457)$ and $X(2632)$ as tetraquark charmed states with open strangeness. In [63] these states are interpreted as a mixture of P-wave quark–antiquark states and four-quark components.

6 Conclusions

We have developed an application and, at the same time, a test for the QCD potential found by means of the AdS/QCD correspondence. We have put it in a semirelativistic wave equation and fitted meson spectra. Our result is that this model, with the AdS/QCD potential plus a contribution from spin interaction, can reproduce the experimental data except for the lighter states (π, K). This agreement has motivated us to make some predictions on the masses of tetraquarks, considering them as bound states of a diquark and an antidiquark. Our conclusions are that some tetraquark states with appropriate flavor content can be identified with the particles $X(3872)$ and $Y(3940)$. On the other hand the present model does not favor the interpretation of some charmed positive parity particles with strangeness as tetraquark states.

Acknowledgement We thank P. Colangelo, F. De Fazio and S. Nicotri for useful discussions and R. Jaffe, L. Maiani, A. Polosa and F. Schöberl for valuable correspondence.

References

1. S. Ricciardi (BaBar Collaboration), AIP Conf. Proc. **892**, 456 (2007)
2. A. Zupanc (Belle Collaboration), AIP Conf. Proc. **892**, 472 (2007)
3. E.S. Swanson, Phys. Rep. **429**, 243 (2006), arXiv:hep-ph/0601110
4. R.L. Jaffe, Phys. Rep. **409**, 1 (2005), arXiv:hep-ph/0409065
5. S.K. Choi et al. (Belle Collaboration), Phys. Rev. Lett. **91**, 262001 (2003), arXiv:hep-ex/0309032
6. D. Acosta et al. (CDF II Collaboration), Phys. Rev. Lett. **93**, 072001 (2004), arXiv:hep-ex/0312021
7. V.M. Abazov et al. (D0 Collaboration), Phys. Rev. Lett. **93**, 162002 (2004), arXiv:hep-ex/0405004
8. B. Aubert et al. (BABAR Collaboration), Phys. Rev. D **71**, 071103 (2005), arXiv:hep-ex/0406022
9. K. Abe et al., arXiv:hep-ex/0505037
10. K. Abe et al., arXiv:hep-ex/0505038
11. K. Abe et al. (Belle Collaboration), Phys. Rev. Lett. **94**, 182002 (2005), arXiv:hep-ex/0408126
12. L. Maiani, F. Piccinini, A.D. Polosa, V. Riquer, Phys. Rev. Lett. **93**, 212002 (2004), arXiv:hep-ph/0407017
13. L. Maiani, F. Piccinini, A.D. Polosa, V. Riquer, Phys. Rev. D **71**, 014028 (2005), arXiv:hep-ph/0412098
14. L. Maiani, V. Riquer, F. Piccinini, A.D. Polosa, Phys. Rev. D **72**, 031502(R) (2005), arXiv:hep-ph/0507062
15. L. Maiani, A.D. Polosa, V. Riquer, arXiv:hep-ph/0707.3354
16. A. De Rujula, H. Georgi, S.L. Glashow, Phys. Rev. D **12**, 147 (1975)
17. P. Colangelo, G. Nardulli, M. Pietroni, Phys. Rev. D **43**, 3002 (1991)
18. E. Eichten, K. Gottfried, T. Kinoshita, K.D. Lane, T.M. Yan, Phys. Rev. D **17**, 3090 (1978). Erratum-ibid. D **21**, 313 (1980)
19. J.L. Richardson, Phys. Lett. B **82**, 272 (1979)
20. W. Buchmuller, S.H.H. Tye, Phys. Rev. D **24**, 132 (1981)
21. O. Andreev, V.I. Zakharov, Phys. Rev. D **74**, 025023 (2006), arXiv:hep-ph/0604204
22. B. Aubert et al. (BABAR Collaboration), Phys. Rev. Lett. **90**, 242001 (2003), arXiv:hep-ex/0304021
23. A.V. Evdokimov et al. (SELEX Collaboration), Phys. Rev. Lett. **93**, 242001 (2004), arXiv:hep-ex/0406045
24. J. Maldacena, Adv. Theor. Math. Phys. **2**, 231 (1998)
25. J. Maldacena, Phys. Rev. Lett. **80**, 4859 (1998)
26. S.-J. Rey, J.-T. Yee, Eur. Phys. J. C **22**, 379 (2001)
27. E. Witten, Adv. Theor. Math. Phys. **2**, 505 (1998)
28. J.A. Minahan, N.P. Warner, J. High. Energy Phys. **9806**, 005 (1998)
29. H. Dorn, H.-J. Otto, J. High. Energy Phys. **9809**, 021 (1998)
30. J. Greensite, P. Olesen, J. High. Energy Phys. **001**, 9904 (1999)
31. N. Drukker, D.J. Gross, H. Ooguri, Phys. Rev. D **60**, 125006 (1999)
32. A.M. Polyakov, V.S. Rychkov, Nucl. Phys. B **581**, 116 (2000)
33. J. Erlich, E. Katz, D.T. Son, M.A. Stephanov, Phys. Rev. Lett. **95**, 261602 (2005), arXiv:hep-ph/0501128
34. A. Karch, E. Katz, D.T. Son, M.A. Stephanov, Phys. Rev. D **74**, 015005 (2006), arXiv:hep-ph/0602229
35. O. Andreev, Phys. Rev. D **73**, 107901 (2006), arXiv:hep-th/0603170
36. P. Cea, G. Nardulli, Phys. Rev. D **34**, 1863 (1986)
37. T. Barnes, S. Godfrey, E.S. Swanson, Phys. Rev. D **72**, 054026 (2005), arXiv:hep-ph/0505002
38. K. Karamcheti, *Principles of Ideal Fluid Aerodynamics* (Wiley, New York, 1966)
39. W.-M. Yao et al. (Particle Data Group), J. Phys. G **33**, 1 (2006)
40. D. Ebert, R.N. Faustov, V.O. Galkin, Phys. Lett. B **634**, 214 (2006), arXiv:hep-ph/0512230
41. D. Ebert, R.N. Faustov, V.O. Galkin, W. Lucha, arXiv:hep-ph/0706.3853
42. D. Ebert, R.N. Faustov, V.O. Galkin, Phys. Rev. D **67**, 014027 (2003), arXiv:hep-ph/0210381
43. R.L. Jaffe, Phys. Rev. D **15**, 281 (1977)
44. R.L. Jaffe, F.E. Low, Phys. Rev. D **19**, 2105 (1979)
45. M.G. Alford, R.L. Jaffe, Nucl. Phys. B **578**, 367 (2000), arXiv:hep-lat/0001023
46. N.A. Tornqvist, Phys. Lett. B **590**, 209 (2004), arXiv:hep-ph/0402237
47. E.S. Swanson, Phys. Lett. B **588**, 189 (2004), arXiv:hep-ph/0311229
48. F.E. Close, P.R. Page, Phys. Lett. B **578**, 119 (2004), arXiv:hep-ph/0309253
49. S. Pakvasa, M. Suzuki, Phys. Lett. B **579**, 67 (2004), arXiv:hep-ph/0309294
50. C.Y. Wong, Phys. Rev. C **69**, 055202 (2004), arXiv:hep-ph/0311088
51. E. Braaten, M. Kusunoki, Phys. Rev. D **69**, 114012 (2004), arXiv:hep-ph/0402177
52. T. Barnes, S. Godfrey, Phys. Rev. D **69**, 054008 (2004), arXiv:hep-ph/0311162
53. B.A. Li, Phys. Lett. B **605**, 306 (2005), arXiv:hep-ph/0410264
54. H. Hogaasen, J.M. Richard, P. Sorba, Phys. Rev. D **73**, 054013 (2006), arXiv:hep-ph/0511039
55. C.W. Bernard et al. (MILC Collaboration), Phys. Rev. D **56**, 7039 (1997), arXiv:hep-lat/9707008
56. Z.H. Mei, X.Q. Luo, Int. J. Mod. Phys. A **18**, 5713 (2003), arXiv:hep-lat/0206012
57. K. Abe et al., arXiv:hep-ex/0507019
58. L. Maiani, A.D. Polosa, V. Riquer, arXiv:hep-ph/0708.3997
59. K. Abe et al. (Belle Collaboration), arXiv:hep-ex/0708.1790
60. B. Aubert et al. (BABAR Collaboration), Phys. Rev. Lett. **95**, 142001 (2005), arXiv:hep-ex/0506081
61. Q. He et al. (CLEO Collaboration), Phys. Rev. D **74**, 091104 (2006), arXiv:hep-ex/0611021
62. C.Z. Yuan et al. (Belle Collaboration), arXiv:hep-ex/0707.2541
63. J. Vijande, F. Fernandez, A. Valcarce, Phys. Rev. D **73**, 034002 (2006). Erratum-ibid. D **74** 059903 (2006), arXiv:hep-ph/0601143